Real-time observation of the effect of iron on receptor-mediated endocytosis of transferrin conjugated with quantum dots

Hai-Li Zhang
Yong-Qiang Li
Ming-Zhen Zhang
Yuan-Di Zhao
Huazhong University of Science and Technology
Wuhan National Laboratory for Optoelectronics
Britton Chance Center for Biomedical Photonics
Wuhan, Hubei 430074
China

Abstract. The optical properties of antiphotobleaching and the advantage of long-term fluorescence observation of quantum dots are fully adopted to study the effects of iron on the endocytosis of transferrin. Quantum dots are labeled for transferrin and endocytosis of transferrin in HeLa cells is observed under the normal state, iron overloading, and an iron-deficient state. In these three states, the fluorescence undergoes a gradual process of first dark, then light, and finally dark, indicating the endocytosis of transferrin. The fluorescence intensity analysis shows that a platform emerges when fluorescence changes to a certain degree in the three states. Experienced a same period of time after platform, the fluorescence strength of cells in the normal state is 1.2 times the first value, and the iron-deficiency state is 1.4 times, but the iron overloading state was 0.85 times. We also find that the average fluorescence intensity in cells detected by the spectrophotometer in the iron-deficiency state is almost 7 times than that in a high iron state. All this proves that iron overloading would slow the process, but iron deficiency would accelerate endocytosis. We advance a direct observational method that may contribute to further study of the relationship of iron and transferrin. © *2010 Society of Photo-Optical Instrumentation Engineers.* [DOI: 10.1117/1.3465595]

Keywords: quantum dots; transferrin; iron; deferoxamine.

Paper 10042R received Jan. 27, 2010; revised manuscript received May 6, 2010; accepted for publication May 19, 2010; published online Aug. 11, 2010.

1 Introduction

Iron is essential to life because it plays important roles in protein metabolism and the physiological activity of a cell. The iron ion is a cofactor of many enzymes that are involved in a number of important physiological functions, including respiration and nucleic acid replication.[1] Deferoxamine is an iron chelating agent. It can combine with a ferric ion at ratio of 1:1 and achieve the formation of an iron-amine complex. Consequently, because it has a high affinity to iron ions, it can cause an iron deficiency in the cellular environment.[2,3] As one element of the enzymes of the ribonucleoside diphosphate reductase coenzyme that catalyze the formation of DNA,[4–6] iron is especially important in cancer and tumors. Human disease would be induced depending on whether its concentration is too high or too low. Therefore, the regulation of iron ion concentration is particularly important. Previous studies showed that iron overloading could promote the growth of tumor cells and iron deficiency could induce apoptosis.[7–11]

Iron was transported into the cell by transferrin through cell surface receptor-mediated endocytosis. Transferrin is a plasma iron-containing protein and can regulate the content of plasma iron. It integrates with the cell surface receptors and iron on the extracellular level, and is transported into the cells. Iron and transferrin protein interactions and their effect on cells have attracted a large number of researchers. One important reason is the overexpression of transferrin receptors in cancer cells, which provides an important method for the identification, diagnosis, and treatment of tumor cells. Thus, it is of great significance in the biomedical field. However, most of such studies use radioisotopes,[12–14] immunocytochemical assay,[15,16] and molecular biology methods.[17,18] Although the application of a radioactive method could provide accurate research data, there are radiological safety issues and the expensive equipment requires professional staff to operate it; immunocytochemical assay generally involves use of commercial agents and costs more; molecular biology tools are the mechanism in the molecular-level studies and cannot achieve intuitive detection.

As a new type of nanocrystals for a fluorescent marker, quantum dots (QDs) have many optical properties, such as the fact that the excitation spectra show a wide and continuous distribution, while the emission spectrum is a narrow and symmetrical distribution.[19–23] For many characteristics, such as adjustable colors, photochemical stability, difficult to break down, and difficult to bleach, they can significantly increase the detection sensitivity and extend the observation time of *in vivo* imaging. Therefore, by avoiding the traditional fluores-

Address all correspondence to: Yuan-Di Zhao, Huazhong University of Science and Technology, Wuhan National Laboratory for Optoelectronics, Britton Chance Center for Biomedical Photonics, Wuhan, Hubei 430074 China. Tel: 86-27-87792235; Fax: 86-27-87792202; E-mail: zydi@mail.hust.edu.cn

cent dyes in biological applications and some of their short-comings, QDs show broad application prospects.[24–26]

Recently, the preparation and application of conjugates of QDs and transferrin have been reported,[27,28] but the influence of iron on the endocytosis process of transferrin has rarely been studied. In this paper, we make full use of antiphotobleaching and the advantage of the long-term fluorescence observation of QDs to study the effects of iron on the endocytosis of transferrin. Fluorescence imaging and spectroscopic analysis show that the transferrin integrated into cells is reduced under a high-iron state, while it increases under an iron deficiency state. These results are consistent with previous works on the radioactive iodine detection method.[29,30] Relatively speaking, this method is not only simpler and intuitive, but also can be used for long-term observation.

2 Materials and Methods

2.1 Materials

CdSe/ZnS QDs were synthesized according to previous reports.[27,28] $FeCl_3$, defetoxamine (DFO), 1-ethyl-3-(3-dimethylaminopropyl) carbodiimide hydrochloride (EDC), and transferrin (Tf) were purchased from Sigma-Aldrich Fine Chemicals (St. Louis, Missouri). A transferrin receptor enzyme-linked immunosorbent assay (ELISA) kit was purchased from R&D Systems (Minneapolis, Minnesota). All other chemicals and materials used in the experiments were of analytical grade and water was deionized.

2.2 Instruments

The following equipment were purchased from the companies indicated in parentheses: a luminescence spectrometer (LS-55, PerkinElmer, Waltham, Massachusetts), a fiber optic spectrometer (QE65000, Ocean Optics, Dunedin, Florida), an inverted fluorescence microscope (IX71, Olympus, Nagano, Japan), a cooled color charge-coupled device (CCD, Pixera Penguin 150CL, San Jose, California), an atomic absorption spectrophotometer (AA-300, Perkin Elmer, Inc., Wellesley, Massachusetts), a microplate reader (ELX808TM, Biotek, Winooski, Vermont), and a UV-VIS spectrophotometer (UV-2550, Shimadzu, Japan).

2.3 Preparation of QDs Probes

The whole process of the conjugation of CdSe/ZnS QDs and Tf (QDs-Tf) included three steps. First, 10 μL EDC (5 mg/mL, pH 7.4) were added to a 40 μL water-soluble CdSe/ZnS QDs solution (1.5×10^{-4} M). The size of QDs was about 5 nm and the carboxylic groups were on the surface. Then the solution was added to 100 μL phosphate-buffered saline (PBS, pH 7.2), followed by 15 min of shaking. The next step was that 75 μL of transferrin solution (2 mg/mL) was added into the mixture, and then the whole solution was further stirred for 2 h at room temperature. The resulting mixture was filtered and QDs-Tf was achieved. The synthesization and purification of QDs-TF was reported in previous reports.[27,28]

2.4 Cell Images

HeLa cells were cultured in Dulbecco's modified Eagle's medium (DMEM), supplemented with 10% fetal bovine serum, 100 mg/mL streptomycin, and 100 U/mL penicillin at 37°C in a humidified atmosphere with 5% CO_2. For imaging, the cells were plated on a glass slide in a 3.5-cm dish. To obtained the high-iron status and the iron-deficient condition, $FeCl_3$ and DFO with the same concentration (50 μmol/L) were added to the dish and maintained in the incubator for 6 h. At this time, the cells were in high-iron status with 50 μmol/L $FeCl_3$. Meanwhile, with 50 μmol/L DFO, the cells were in iron-deficient condition. Following that, the cells were washed three times with PBS (pH 7.2), which was pre-incubated at 37°C to remove the growth medium; $FeCl_3$; and DFO. Then fresh DMEM medium with QDs-Tf were added in the dish. Cells were incubated for 15 min at 37°C. This was followed with extensive washing (3 times, 5 min/time) in PBS ice. Finally the treated cells were detected by an IX71 inverted fluorescence microscope with a cooled color CCD. The spectra were recorded by the spectrometer.

2.5 ELISA for Transferrin Receptor

After being plated in 96 wells for 24 h, HeLa cells were washed with fresh medium, and treated with $FeCl_3$ (50 μmol/L) and DFO (50 μmol/L) for 6 h, respectively. The cells were washed three times with PBS. The cells were fixed for 10 min by 0.25% glutaraldehyde at room temperature, washed three times with warm PBS, and closed by 2% bovine serum albumin for 10 min. The expression of transferrin receptor (TfR) in the cells was detected by the ELISA kit. Finally the absorbance of each pore was detected at a wavelength of 450 nm in the ELISA meter. In this study, the data were from four independent experiments.

2.6 Determination of Iron Amount after It Was Transferred into the Cell through the Endocytosis

After HeLa cells were plated in 96-well microtiter plates for 24 h, the experiment was divided into three groups: the normal group, the $FeCl_3$ group, and the DFO group. There were two wells in each group with three repeats. First, in the $FeCl_3$ group, the cells were exposed to 50 μmol/L $FeCl_3$ for 6 h; 50 μl Tf-QDs was added to one of the wells after $FeCl_3$ was washed out at an incubation time of 6 h, and incubated for another 15 min. Second, in the DFO group, 50 μmol/L DFO was added in one well for 6 h, while 50 μl Tf-QDs was added to another well and incubated at 37°C, 5% CO_2 for 15 min after DFO was washed out at the incubation time of 6 h. Third, in the normal cell group, the wells were incubated for 6 h without $FeCl_3$ and DFO, then one of them was exposed to 50 μl Tf-QDs for more 15 min after washing three times with PBS. Finally, all the cells were washed with cold stripping buffer (200 mM NaCl, 50 mM MES, 1 mM $MgCl_2$, 1 mM $CaCl_2$) for 2×2 min to wash out Tf-QDs stained on the plasma membrane. Then the cells were crashed by the cold cell lysis buffer and centrifugated to be collected. The iron concentration was detected by an AA-300 atomic absorption spectrometer (wavelength, 248.3 nm; width of slit, 0.4 mm). The content of intracellular iron which was transferred into cells by TfR was the amount in the wells with Tf-QDs minus that in the wells without Tf-QDs.
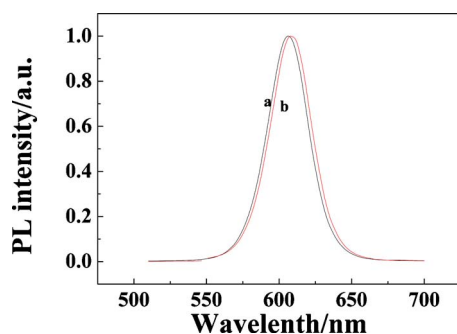
Fig. 1 Fluorescence spectra of (a) QDs and (b) QDs-Tf.

Fig. 3 Fluorescence (FL) intensity changes of cells in the process of endocytosis under the normal physiological condition.

3 Results and Discussion

3.1 Characterization of QDs Probes

The conjugation of QDs-Tf and their purification have been reported.[27,28] In this study, the fluorescence spectra of QDs and QDs-Tf were measured. As shown in Fig. 1, photoluminescent (PL) quantum yields (QYs) were 26 and 18%, respectively, for QDs and QDs-Tf. A red shift was observed in QDs-Tf. We found that 606 nm (before conjugation) moved to 608 nm (after conjugation), and the half-peak width broadened (from 31 into 33 nm), which was possibly due to the combination with Tf to make larger QDs, and the number of Tf binding on the QD surfaces might be also inconsistent, so that size distribution of QDs-Tf increased, leading to a red shift and a half-wavelength width extension.

3.2 Imaging and the Fluorescence Intensity Changes of Cells in the Normal Physiological Condition

To compare the effects of iron deficiency and an iron-rich environment on Tf endocytosis, the QDs-Tf endocytosis process of tumor cells was observed first. The cells were incubated with QDs-Tf at 37°C for 15 min, and then washed three times quickly. Immediately, the whole process of endocytosis was recorded through the Olympus IX71 inverted fluorescent microscope and CCD. The time for the first photograph was set as $t=0$. As shown in Fig. 2, at the beginning, only localized fluorescence appeared in QDs-Tf incubated cells. Then some intermittent fluorescence could be seen on the membrane. Gradually, the fluorescence on the cell mem-
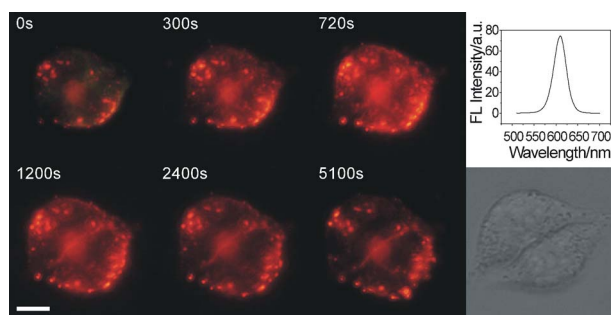

Fig. 2 Video showing bright-field imaging, fluorescence imaging, and fluorescence spectroscopy of the process of receptor-mediated endocytosis of QDs-Tf under the normal physiological condition. Scale bar: 5 μm. (QuickTime, 77.5 KB). [URL: http://dx.doi.org/10.1117/1.3465595.1].
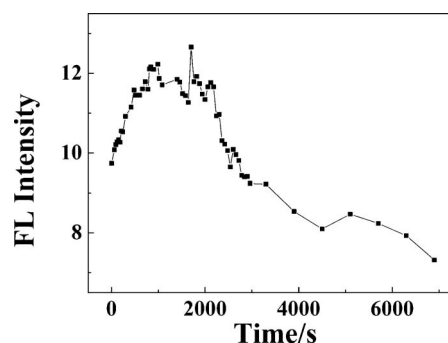
brane increased in brightness, while the punctate fluorophores piled up in the cytoplasm of the cells. Fluorescence throughout the cells grew to be the brightest at around 700 to 800 s followed by gradually weakening. The fluorescence of the cytoplasm clearly dimmed, while the fluorescence of the membrane was still relatively bright at 5100 s. The video in Fig. 2 also provides a description of the entire endocytosis process.

To study the time-varying characteristics of cell fluorescence intensity, the total fluorescence intensity in cells was calculated. Figure 3 shows that the change of the fluorescence intensity of cells was consistent with the images. It went through a process transmitted from dark to the light and then to dark again. This is so because the surface of all living cells have TfRs. In the neutral pH environment, the TfR can bind protein and go into cells by endocytosis. In an acidic intracellular environment, Tf releases iron, after which it goes back to the plasma membrane together with the receptor. In the extracellular neutral environment, the Tf is dissociated from the receptor and freely combines with ferric ion again. Then a new cycle begins again.[31] Therefore, the transfer of Tf for iron ion is different from other receptor-mediated endocytosis processes because its ligand (Tf) and receptor are recycled, and only the iron ion is transported and stored. If the QDs are coupled with Tf protein, they are also involved in the cycle. In the experiments, QDs-Tf was added in the cell culture medium for a certain period of time, after three rinses, and the free probes had already been washed off. In this case, QDs-Tf has undergone combination with the cell membrane receptor and endocytosis into the cell. After the release of iron ions, they also returned to the cell membrane. In this cycle process, QDs have also been transferred from the cell membrane into the cytoplasm, and then back to the membrane, so the cell membrane could be observed to have a very strong fluorescence (Fig. 2). In this process, there is the puzzling phenomenon that, after the free probe are washed off, although a certain amount of QDs probes are maintained, changes in fluorescence was observed in the cells. While fluorescence spectra emission peaks are at 610 nm (Fig. 2), which is very consistent with QDs-Tf (Fig. 1, curve b), indicating that fluorescence indeed resulted from the QDs. This phenomenon was also observed by Lidke et al. using QDs as a probe to detect epidermal growth factor signal transduction,[32] but the reason is not yet clear.

At the same time, pure QDs instead of Tf-QDs were used to label HeLa cells in the same method as a control. After the
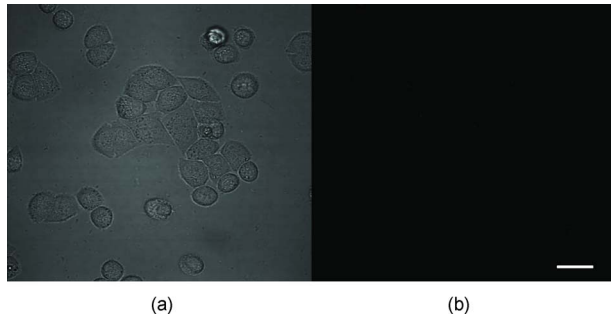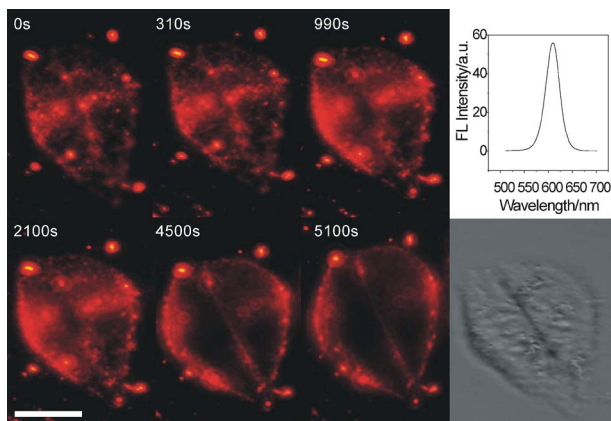
Fig. 4 (a) Bright-field images and (b) fluorescence images of HeLa cells labeled with pure QDs. Scale bar: 5 μm.

Fig. 6 Fluorescence intensity changes of cells in the process of endocytosis under an iron-rich condition.
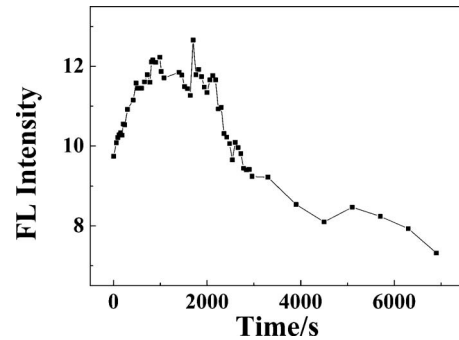
same incubation time and being washed as before, photos of the treated cells were taken. As shown in Fig. 4, no obvious QD fluorescence was observed and only few fluorescent dots appeared in cells and their structure was not clear [Fig. 4(b)]. These images show that unlabeled QDs did not enter the cells in the experiment. This indicates that only Tf-QDs were recognized by the TfR and bound on the membrane and delivered into the cytoplasm after incubation by the TfR. The specificity of endocytosis was also proved in our previous reports.[27]

3.3 Imaging and the Fluorescence Intensity Changes of Cells in an Iron-Rich Condition

From the fluorescence imaging, we observed that when the system contained an excessive level of iron, the fluorescence of the cells also experienced a change from dark to light then to dark (Fig. 5); fluorescence intensity within the plasma membrane reached the maximum in about 2100 s. After the rapid decline in fluorescence intensity, the fluorescence at about 5100 s was not as good as in the beginning state. The video in Fig. 5 also provides a description of the entire process of endocytosis of QDs-Tf under an iron-rich condition. Calculation of fluorescence intensity (Fig. 6) also confirmed this observation. The results showed that when an increase in iron occurs, Tf endocytosis slows down significantly. This

may be because the intracellular iron concentration can affect the TfR mRNA stability. In an iron-rich environment, the stability of TfR mRNA was reduced, the synthesis of receptors was blocked, and expression in cells was depressed.[29,33] Thus, QDs-Tf could not combine with more receptors and the cycle of the Tf also slowed.

3.4 Imaging and the Fluorescence Intensity Changes of Cells in an Iron-Deficient Condition

Different from the preceding studies, the results showed that, after being washed off, free QDs and unlabeled compounds, at 0 s, the cell membrane and the cytoplasm has a strong fluorescence (Fig. 7). Although the fluorescence intensity also showed the transfer from weak to strong then weak process, parts of the cytoplasm has a very strong fluorescence; even at 5100 s, very strong fluorescence was still observed (Fig. 7). The video in Fig. 7 also provides a description of the entire process of endocytosis of QDs-Tf under an iron deficient condition. We deduced that the inside and outside exchanges on the membrane were quite frequent, and the transport of transferring iron was faster. The fluorescence intensity (Fig. 8) also similarly confirmed this observation. This might be due to the increased demand for cells because of the iron ion deficiency, the mRNA stability of the TfR increased, and receptor synthesis was accelerated, leading to an increase of membrane

Fig. 5 Video showing bright-field imaging, fluorescence imaging, and fluorescence spectroscopy of the process of receptor-mediated endocytosis of QDs-Tf under an iron-rich condition. Scale bar: 5 μm. (QuickTime, 214 KB). [URL: http://dx.doi.org/10.1117/1.3465595.2].
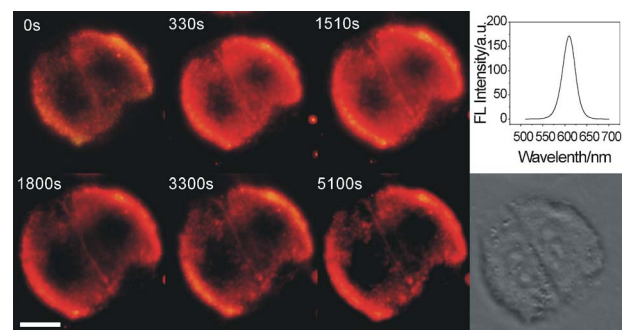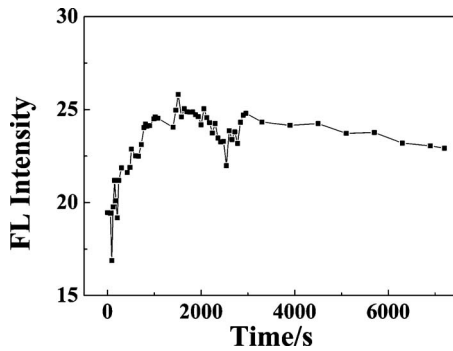

Fig. 7 Video showing bright-field imaging, fluorescence imaging, and fluorescence spectroscopy of the process of receptor-mediated endocytosis of QDs-Tf under an iron-deficient condition. Scale bar: 5 μm. (QuickTime, 154 KB).
[URL: http://dx.doi.org/10.1117/1.3465595.3].

Fig. 8 Fluorescence intensity changes of cells in the process of endocytosis under an iron-deficient condition.

Fig. 9 Fluorescence intensity of cells in three kinds of situations: curve a, a normal condition; curve b, an iron-rich condition; and curve c, an iron deficiency condition.

receptors, so that Tf endocytosis process was accelerated.[34] This was embodied in the cell imaging results—the cell fluorescence intensity was enhanced.

3.5 Fluorescent Intensity Analysis

Comparison of Figs. 3, 6, and 8 shows that after rising to the maximum, the average fluorescence intensities of several cells lasted for different platform times, which were 892 to 2090 s in Fig. 3. At 4092 s, the cell's fluorescence intensity reduced to the maximum 86.4%, but still was 1.2 times that at start point ($t=0$). Under the high-valence iron condition, Fig. 6 displayed the platform of a long period from 710 to approximately 2178 s, when the time for a further period of 2000 s, the cell fluorescence intensity had dropped to the 65.6% of highest intensity, and was only 0.85 times of the initial value ($t=0$). However, in the iron-deficiency state in Fig. 8, the fluorescence intensity of cells from platform terminal (2070 s) to 4070 s, hardly changed. The strength reduced only 4.7% and its fluorescence value approximately was 1.4 times of the initial value; even after 3200 s, when time was at 7200 s, the fluorescence intensity reduced to only 90.6% of the maximum, and was still 1.3 times the initial value. Therefore, we concluded that the high-iron and iron-deficiency states have different effects on the Tf endocytosis process, which slowed under a high-valence iron condition and accelerated with low iron reserves.

To more clearly understand the effect of iron on receptor-mediated endocytosis of Tf, fluorescence spectra of whole-cells in three cases were obtained. HeLa cells were treated as already discussed. After the cells were labeled with Tf-QDs in an iron-overloading environment, an iron-deficiency environment, and a normal state, they were washed and centrifuged to collect them. The fluorescence intensity was measured immediately. As the result shown in Fig. 9 demonstrates, the highest fluorescence peaks were about 607 nm, indicating that the fluorescence was generated by QDs. The fluorescence intensity was maximal under the iron-deficiency condition, while the minimal was observed under an iron-rich condition. The results of fluorescence spectra coincided with our already presented results. In an iron-rich environment, TfR synthesis was blocked, membrane binding to Tf fell off relatively, and thus the fluorescence intensity was lowest. The cells were in a hard iron-flaw condition while DFO acted on the cell; to reduce the harm to themselves, cells speeded the iron ion transport.
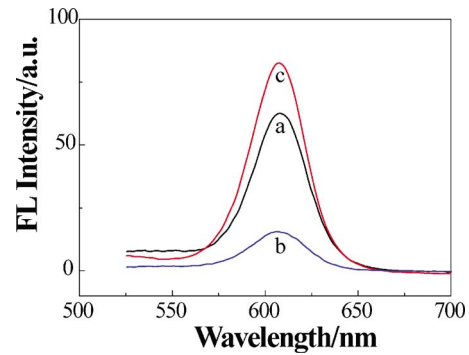
Therefore, the cytomembrane acceptor synthesis increased, the transferrin binding to the receptor on the cell relatively increased in the number, and the fluorescence intensity strengthened as well.

3.6 TfR Amount and Intracellular Iron Content Transferred into Cells by TfR among Different Environments

In our experiment, the whole process of fluorescence changes in cells was detected among different environments. When the fluorescence signal varied, ion concentration had also changed in fact. While the ion concentration changes could be detected by chemical methods. ELISA and atom absorption spectrum analysis were used to study the biological effects of different iron concentrations on the expression of TfR and the content of intracellular iron transferred by TfR through endocytosis. The results revealed that when the cells were incubated with 50 μmol/L DFO, the TfR was about 1.25 nmol/L, which was almost twice than in medium with 50 μmol/L FeCl$_3$ (Table 1). The expression of TfR on HeLa cells becomes lower with an increase of the iron element in the experiment. In an iron-deficiency environment, the amount of iron transferred into cells by TfRs was the highest, which was almost 4 times that in the high-iron status and three times that in a normal status. In contrast, in a high-iron environment, the iron ion uptake by cells through endocytosis was the least (Table 1). The results coincided with previous reports, which showed that the expression of TfR was relevant to the need for iron in cells.[35] Moreover, when the cells were in an iron-deficiency condition, the TfR mRNA expression increased.[33] The amount of TfR decreased when iron increased.[29]

Table 1 TfR amount and iron content transferred into cells by TfR among different environments.

Group	Iron Content Transferred into Cells (mg/L×10⁴ cells)	TfR (nmol/L×10⁴ cells)
FeCl$_3$-50	0.010±0.004	0.65±0.12
Normal	0.012±0.003	0.98±0.15
DFO-50	0.039±0.005	1.25±0.07

4 Conclusion

Iron plays an important role in the biological body, but the mechanism of its transport is not yet clear. we used optical imaging and spectral analysis to study the biological effects of iron-deficiency and iron-rich environments on receptor-mediated Tf. The results indicated that the transportation of iron was slowed in the high-iron status, while it sped up in iron deficiency. The research method is simple and convenient. The fluorescence characteristic property of QDs was fully utilized, such as antibleaching and long-term observation. This provided a new way to study transportation of iron and has evident biological significance.

References

1. N. T. V. Le and D. R. Richardson, "The role of iron in cell cycle progression and the proliferation of neoplastic cells," *Biochim. Biophys. Acta* **1603**(1), 31–46 (2002).
2. S. N. Rubtsova and Y. M. Vasil'ev, "Iron chelator deferoxamine induces epithelial transformation of tumor cells," *Dokl. Biol. Sci.* **411**(1), 517–519 (2006).
3. A. I. Schafer, S. Rabinowe, M. S. Le Boff, K. Bridges, R. G. Cheron, and R. Dluhy, "Long-term efficacy of deferoxamine iron chelation therapy in adults with acquired transfusional iron overload," *Arch. Intern Med.* **145**(7), 1217–1221 (1985).
4. P. Ponka, C. Beaumont, and D. R. Richardson, "Function and regulation of transferrin and ferritin," *Semin Hematol.* **35**(1), 35–54 (1998).
5. D. R. Richardson and P. Ponka, "The molecular mechanisms of the metabolism and transport of iron in normal and neoplastic cells," *Biochim. Biophys. Acta* **1331**(1), 1–40 (1997).
6. R. R. Crichton and M. Charloteaux-Wauters, "Iron transport and storage," *Eur. J. Biochem.* **164**(3), 485–506 (1987).
7. E. D. Weinberg, "Iron therapy and cancer," *Kidney Int.* **55**, sl31–s134 (1999).
8. H. Rezazadeh and M. Atha, "Effect of iron overload on the benzoyl peroxide-mediated tumor promotion in mouse skin," *Cancer Lett.* **126**, 135–142 (1998).
9. G. Bhasin, H. Kausar, M. S. Alam, and M. Athar, "Progressive iron overload enhances chemically mediated tumor promotion in murine skin," *Arch. Biochem. Biophys.* **409**, 262–273 (2003).
10. S. Kotamraju, C. R. Cjotambar, S. V. Kalivendi, J. Joseph, and B. Kalyanaraman, "Transferrin receptor-dependent iron uptake is responsible for doxorubicin-mediated apoptosis in endothelial cells: role of oxidant-induced iron signaling in apoptosis," *J. Biol. Chem.* **277**(12), 17179–17187 (2002).
11. K. Murakami, K. Ishida, K. Watakabe, R. Tsubouchi, M. Naruse, and M. Yoshino, "Maltol/iron-mediated apoptosis in HL60 cells: participation of reactive oxygen species," *Toxicol. Lett.* **161**(2), 102–107 (2006).
12. Z. Wei and Y. Zhang, "Experimental study of transferrin receptor molecular imaging in human hepatocellular carcinoma transplanted in nude mice," *Zhong Hua Zhong Liu Za Zhi* (Chin. J. Oncol.) **28**(2), 96–98 (2006).
13. E. H. Morgan and T. C. Appleton, "Autoradiographic localization of 125I-labelled transferrin in rabbit reticulocytes," *Nature* **223**, 1371–1372 (1969).
14. R. Adler, E. Hurwitz, J. R. Wands, M. Sela, and D. Shouval, "Specific targeting of adriamycin conjugates with monoclonal antibodies to hepatoma associated antigens to intrahepatic tumors in athymic mice," *Hepatology (Philadelphia, PA, U. S.)* **22**(5), 1482–1487 (2005).
15. W. Dong, J. Wang, and J. Zhang, "Establishment and application for detection of TfR of rat bone marrow cells by immunocytochemical method," *J. Medern Lab. Med.* **18**(5), 11–12 (2003).
16. R. Sciot, A. C. Paterson, P. Eyken, F. Callea, M. C. Kew, and V. J. Desmet, "Transferrin receptor expression in human hepatocellular carcinoma: an immunohistochemical study of 34 cases," *Histopathology* **12**(1), 53–63 (1988).
17. M. B. Gangloff, C. Lai, D. R. Van Campen, D. D. R. Miller, W. A. Norvell, and R. P. Glahn, "Ferrous iron uptake but not transfer is down-regulated in Caco-2 cells grown in high iron serum-free medium," *J. Nutr.* **126**(12), 3118–3127 (1996).
18. G. Xu, R. Liu, O. Zak, P. Aisen, and M. R. Chance, "Structural allostery and binding of the transferrin receptor complex," *Mol. Cell Proteomics* **4**(12), 1959–1967 (2005).
19. L. Melton, "Imaging: the big picture," *Nature* **437**, 775–779 (2005).
20. W. C. W. Chan, D. J. Maxwell, X. Gao, R. E. Bailey, M. Han, and S. Nie, "Luminescent quantum dots for multiplexed biological detection and imaging," *Curr. Opin. Biotechnol.* **13**(1), 40–46 (2002).
21. W. C. W. Chan and S. Nie, "Quantum dot bioconjugates for ultrasensitive nonisotopic detection," *Science* **281**, 2016–2018 (1998).
22. A. Douplik, A. Zam, R. Hohenstein, A. Kalitzeos, E. Nikenke, and F. Stelzle,"Limitations of cancer margin delineation by means of autofluorescence imaging under conditions of laser surgery," *J. Innov. Opt. Health Sci.* **1**, 45–51 (2010).
23. A. P. Alivisatos, W. Gu, and C. Larabell, "Quantum dots as cellular probes," *Annu. Rev. Biomed. Eng.* **7**, 55–76 (2005).
24. J. H. Wang, H. Q. Wang, H. L. Zhang, X. Q. Li, X. F. Hua, and Y. D. Zhao, "Purification of denatured bovine serum albumin coated CdTe quantum dots for sensitive detection of silver(I) ions," *Anal. Bioanal. Chem.* **388**(4), 969–974 (2007).
25. X. F. Hua, T. C. Liu, Y. C. Cao, B. Liu, H. Q. Wang, J. H. Wang, and Y. D. Zhao, "Characterization of the coupling of quantum dots and immunoglobulin antibodies," *Anal. Bioanal. Chem.* **386**(6), 1665–1671 (2006).
26. H. Q. Wang, T. C. Liu, Y. C. Cao, Z. H. Huang, J. H. Wang, and Y. D. Zhao, "A flow cytometric assay technology based on quantum dots-encoded beads," *Anal. Chim. Acta* **580**(1); 18–23 (2006).
27. H. Q. Wang, H. L. Zhang, X. Q. Li, J. H. Wang, Z. L. Huang, and Y. D. Zhao, "Solubilization and bioconjugation of QDs and their application in cell imaging," *J. Biomed. Mater. Res. Part A* **86**(3), 833–841 (2008).
28. T. C. Liu, J. H. Wang, H. Q. Wang, H. L. Zhang, Z. H. Zhang, X. F. Hua, Y. C. Cao, Y. D. Zhao, and Q. M. Luo, "Bioconjugate recognition molecules to quantum dots as tumor probes," *J. Biomed. Mater. Res. Part A* **83**(4), 1209–1216 (2007).
29. J. H. Ward, J. P. Kushner, and J. Kaplan, "Regulation of HeLa cell transferrin receptors," *J. Biol. Chem.* **257**, 10317–10323 (1982).
30. F. Louache, U. Testa, P. Pelicci, P. Thomopoulos, M. Titeux, and H. Rochant, "Regulation of transferrin receptors in human hematopoietic cell lines," *J. Biol. Chem.* **259**, 11576–11582 (1984).
31. A. Dautry-Varsat, A. Ciechanover, and H. F. Lodish, "pH and the recycling of transferrin during receptor-mediated endocytosis," *Proc. Natl. Acad. Sci. U.S.A.* **80**, 2258–2262 (1983).
32. D. S. Lidke, P. Nagy, R. Heintzmann, D. J. Arndt-Jovin, J. N. Post, H. E. Grecco, E. A. Jares-Erijman, and T. M. Jovin, "Quantum dot ligands provide new insights into erbB/HER receptor-mediated signal transduction," *Nat. Biotechnol.* **22**(2), 198–203 (2004).
33. U. Testa, F. Louache, M. Titeux, P. Thomopoulos, and H. Rochant, "The iron-chelating agent picolinic acid enhances transferrin receptors expression in human erythroleukaemic cell lines," *Br. J. Haematol.* **60**, 491–502 (1985).
34. B. Vaisman, E. Fibach, and A. M. Konijn, "Utilization of intracellular ferritin iron for hemoglobin synthesis in developing human erythroid precursors," *Blood* **90**(2), 831–838 (1997).
35. E. C. Theil, "Regulation of ferritin and transferrin receptor mRNAs," *J. Biol. Chem.* **265**, 4771–4774 (1990).